



Deposited via The University of Sheffield.

White Rose Research Online URL for this paper:

<https://eprints.whiterose.ac.uk/id/eprint/133901/>

Version: Published Version

Article:

Al Zamzami, I., Di Cocco, V., Davison, J.B. et al. (2018) Static strength and design of aluminium-to-steel thin welded joints. *Welding in the World*, 62 (6). pp. 1255-1272. ISSN: 0043-2288

<https://doi.org/10.1007/s40194-018-0634-2>

© The Author(s) 2018. This article is distributed under the terms of the Creative Commons Attribution 4.0 International License (<http://creativecommons.org/licenses/by/4.0/>), which permits unrestricted use, distribution, and reproduction in any medium, provided you give appropriate credit to the original author(s) and the source, provide a link to the Creative Commons license, and indicate if changes were made.

Reuse

This article is distributed under the terms of the Creative Commons Attribution (CC BY) licence. This licence allows you to distribute, remix, tweak, and build upon the work, even commercially, as long as you credit the authors for the original work. More information and the full terms of the licence here:

<https://creativecommons.org/licenses/>

Takedown

If you consider content in White Rose Research Online to be in breach of UK law, please notify us by emailing eprints@whiterose.ac.uk including the URL of the record and the reason for the withdrawal request.



Static strength and design of aluminium-to-steel thin welded joints

I. Al Zamzami¹ · V. Di Cocco² · J. B. Davison¹ · F. Iacoviello² · L. Susmel¹ 

Received: 29 December 2017 / Accepted: 26 July 2018
© The Author(s) 2018

Abstract

Welding together dissimilar materials, and, in particular, aluminium alloys to steel, has always been a challenge because of the significant difference in their mechanical, thermo-physical and metallurgical properties which causes the formations of hard and brittle intermetallic phases in the welding region. Recently, EWM® has developed a welding process known as ColdArc®, where the heat input and arc stability are precisely controlled. The present study was designed to investigate the static strength of aluminium-to-steel thin welded joints manufactured using EWM coldArc® welding technology. Butt, lap and cruciform welded connections were prepared to assess tensile strength and failure mode of these hybrid welded joints. The visual examination of the fracture surfaces revealed that, regardless of the geometry of the welded connections, the fracture of the joints always took place in the heat-affected zone (HAZ) on the aluminium side. This inspection indicated that the use of EWM coldArc® welding technology had improved the strength of the hybrid welded joint significantly and removed the problem of having a brittle phase in the welding zone. The results obtained from this investigation shows that Eurocode 9 can also be used to design aluminium-to-steel thin welded joints.

Keywords Hybrid joints · coldArc · Heat-affected zone · Fracture · Eurocode 9

Nomenclature

σ_{Ed}	Design normal stress, perpendicular to the weld axis
τ_{Ed}	Design shear stress, parallel to the weld axis
σ_{eq}	Combined normal and shear stresses
f_w	Characteristic strength of the weld metal
γ_{Mw}	Partial safety factor for welded joints
$\sigma_{eq, fillet}$	Combined normal and shear stresses for fillet welds
σ_{\perp}	Direct stress perpendicular to the weld throat
τ_{\perp}	Shear stresses perpendicular to the fillet weld
τ_{\parallel}	Shear stresses parallel to the fillet weld

1 Introduction

To increase their competitiveness in the market, one of the most difficult challenges faced by companies designing and manufacturing metallic components and structures of all kinds is improving their performance by reducing not only the weight but also the associated production, energy and maintenance costs. In this context, driven by tightening legislation, customer demands and competitive pressures, it is also necessary to reduce carbon emissions and usage of natural resources. For instance, many government policies have been established to lower the carbon dioxide emissions from the land transportation. Therefore, the transportation industry has been challenged to reduce the fuel consumption. In addition to fuel-efficient engines, mass efficient structural materials are required to reduce the total weight of the vehicles [1, 2].

One of the most difficult aspects associated with design and fabrication of a high-performance mechanical assembly is efficiently joining together its different parts. The most critical issue associated with the use of modern, advanced composite materials to manufacture complex lightweight hybrid structures is that joining composites to other composites as well as to other structural materials which is neither simple nor cheap. In contrast, metallic materials can efficiently be joined together at a relatively low cost by welding. For this reason,

Recommended for publication by Commission X - Structural Performances of Welded Joints - Fracture Avoidance

✉ L. Susmel
l.susmel@sheffield.ac.uk

¹ Department of Civil and Structural Engineering, The University of Sheffield, Mappin Street, Sheffield S1 3JD, UK

² Università di Cassino e del Lazio Meridionale, DiCeM, via G. Di Biasio 43, Cassino, FR, Italy

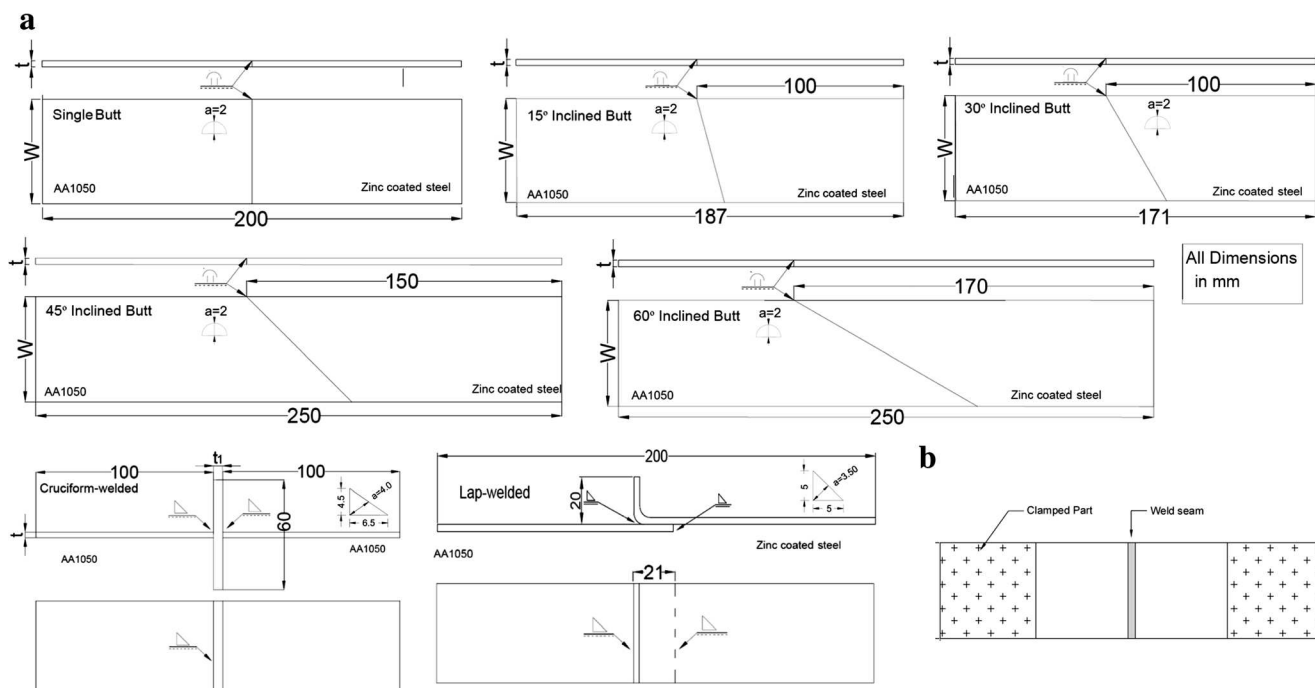


Fig. 1 Geometry of the investigated aluminium-to-steel welded components (a). Schematisation of the tensile specimens (b)

manufacturing structures and components by metallurgically welding aluminium to steel represents an innovative solution for the fabrication of future low-cost and environmentally friendly lightweight structural assemblies.

Accordingly, in recent years, the issue of joining aluminium to steel has received considerable attention. The main problem associated with the use of conventional fusion welding technologies to weld aluminium to steel is that these two materials have different physical properties (e.g. thermal expansion, conductivity and melting temperature). Furthermore, their different metallurgical characteristics lead to the formation of hard and brittle intermetallic phases (such

as Fe-Al) at the interface between the two materials, with these intermetallic phases markedly deteriorating the mechanical properties of the welded connections [1, 3]. In this context, certainly explosion-bonding represents an effective technology allowing both similar and dissimilar materials to be joined together. This process was developed in the late 1950s in the shipbuilding industry to weld aluminium to steel so that connections with improved corrosive, mechanical and strength properties could be manufactured effectively. The drawback of this method is that dis-bonding is likely to occur during construction and in-service operations, with this resulting in extra time and costs associated with repairing/removing [4, 5].

Fig. 2 Current and voltage of the EWM coldArc process and the standard short arc process

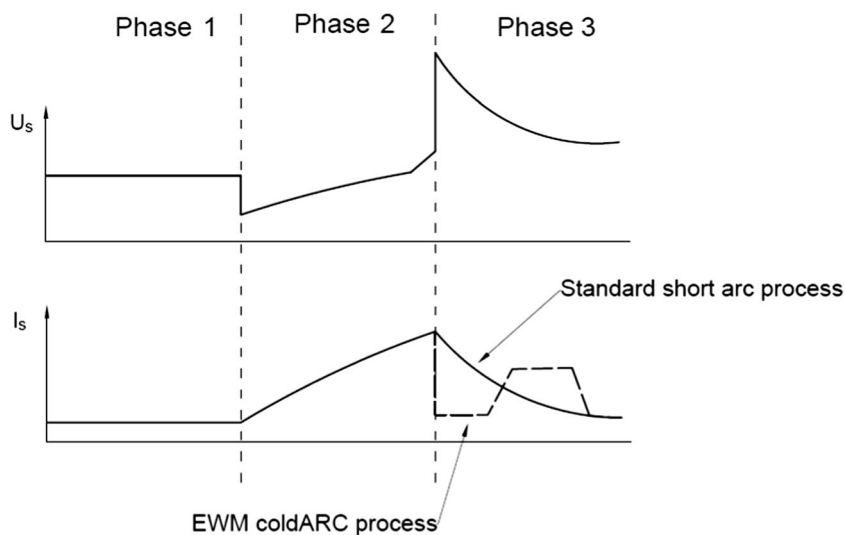




Fig. 3 Spatter-free welding achieved by using EWM coldArc welding technology

In order to overcome the above problems, over the past decade, there has been a remarkable increase in the research work done in the dissimilar metal welding field with the aim not only of achieving stronger and more flexible hybrid welded joint solutions but also of increasing manufacturing productivity [6–9].

Owing to the intrinsic limitations of explosion-bonding, in recent years, different attempts have been made to explore alternative technological solutions. For instance, Fukumoto [10] used the friction welding process to manufacture hybrid welded joints made of 5052 aluminium alloy and 304 stainless steel. This investigation shows that longer friction time causes the formation of intermetallic layers at the weld interfaces. Further, as the intermetallic layer thickness increases, the connections become more and more brittle, with fracture occurring at the weld interface [10].

Friction stir welding (FSW) is another joining process that has been used to manufacture aluminium-to-steel connections, with FSW being used to manufacture mainly lap and butt joints. These investigations demonstrate that, as far as FSW is concerned, the joint strength tends to increase as the rotation speed increases but decrease as the travelling speed increases [1, 4, 11, 12]. Lately, this process was further developed so that aluminium-to-steel welded joints could be manufactured using a multi-pass welding strategy. The results obtained

using FSW show that the use of this technology leads to the elimination of the intermetallic layers, with this resulting in an increase of the overall strength of the joints. The main disadvantage of this method is that friction stir welded connections are characterised by a non-uniform distribution of the mechanical properties across the weld [13].

Laser welding-based processes have proven to be very effective in welding aluminium to steel, their use resulting in a reduction of the microstructural damage at the interface associated with the presence of intermetallic compound (IMC) layers. With this joining technology, good results can be obtained provided that the temperature at the interface is controlled during welding so that the growth of the IMC layers is limited [2, 5, 14]. Gao [15] suggested that the interface temperature should be lower than 1120 °C.

Examination of the state of the art suggests that the main challenges to be faced when welding aluminium to steel are as follows: (i) minimising the presence of IMC layers at the interface, (ii) controlling the thickness of IMC layers to avoid the formation of brittle phases, and (iii) preventing the formation of pores and cracks which lower the overall strength of aluminium-to-steel welded joints. As a result, a variety of low-energy-input welding technologies were developed in recent years to join aluminium to steel effectively [16, 17]. In this context, EWM coldArc® undoubtedly represents the most advanced technological solution that is available in the market to date (www.ewm-group.com).

In this complex and challenging scenario, the goal of the present study is to investigate the static strength of hybrid welded joints manufactured using the EWM coldArc® welding technology with the aim of proposing safe assessment rules to be used in situations of practical interest to design aluminium-to-steel welded joints against static loading.

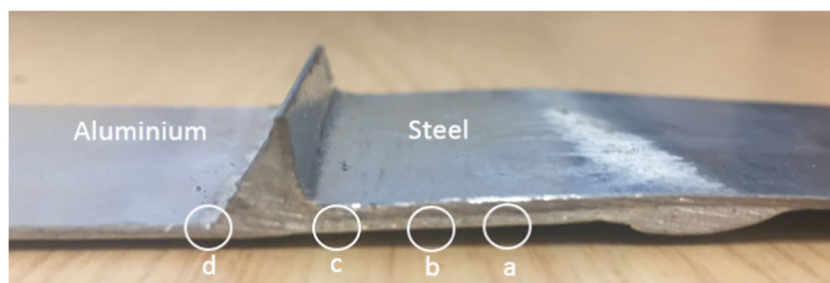
2 The EWM ColdArc® welding technology

The EWM coldArc® welding technology was used in this investigation to weld thin aluminium alloys to galvanised steel sheets (Fig. 1) with a thickness of 1 mm. It is an advanced form of welding that allows an excellent control over the rate of heat input and the metal transfer. Its lower heat input

Table 1 Mass chemical composition of the used materials by weight percentage

Alloy	Chemical composition [wt%]							
	Cu	Mg	Si	Fe	Mn	Zn	Ti	Al
AA1050	0–0.05	0–0.05	0.25	0–0.4	0.05	0.07	0–0.05	Balanced
EN10130:199	0.12	0.045	0.045	0.60	Balanced			
AA4043	0.01	0.05	4.5–6.0	0.80	0.05	0.1	0.2	Balanced

Fig. 4 Position of the investigated sections in the aluminium-to-steel welded joints for the metallurgical analyses



enables welding professionals to weld thin metal sheets without causing any burn through. It can join thin sheets from 0.3 mm using automated welding machine and from 0.7 mm using manual welding machine [18].

It is a modified short arc process for root welding of pipes or thin materials and has excellent gap bridging capabilities. Due to the low heat used during the process, it causes no damage to the zinc coating and less warping. Therefore, it is an ideal solution to weld aluminium to steel, provided that the steel sheet is coated with zinc which minimises the formation of the hard and brittle intermetallic phases [18, 19].

Figure 2 compares the welding current, I_s , and voltage, U_s , of the coldArc welding process and traditional short arc

welding. This figure shows that the first two phases are the same. However, the advantage of the coldArc process is shown in phase 3 at the moment of the arc re-ignition and immediately afterwards. In particular, at the moment of the arc re-ignition, the output is considerably lower. Moreover, there is a reduction in the output shortly after the arc ignites which occurs in an exceptionally dynamic and controlled way. After the stabilisation of the arc, there is a slight increase in the current for a defined short period of time, known as melt pulse, to create regular separations [18].

A widespread occurrence in the inert metal gas (MIG) welding is the formation of spatter which is essentially droplets of molten materials generated around or on the weld seam. The problem of having spatter during welding is that it is a material waste and it requires more time to clean it up. Another advantage of using the coldArc® welding process is that a spatter-free weld is achievable (see Fig. 3), due to the power reduction during the arc re-ignition.

It is worth mentioning here also that the welding parameters are optimised and integrated into the machine programme provided by welding company EWM. By choosing the correct programme code from the list provided and set the thickness of the material, the machine will set up the corresponding welding parameters accordingly. If required, the welding parameters can be adjusted manually.

3 Experimental procedure

The experimental work presented here was designed to investigate the reliability of the EWM coldArc® welding process in joining thin sheets of aluminium alloy to galvanised steel with various joints configurations (Fig. 1). The test specimens used in this investigation were welded manually by an experienced welding technician using EWM alpha Q551 pulse machine. The materials used were 1-mm-thick aluminium alloy AA1050 and zinc-coated cold rolled low-carbon steel EN10130:199 (1-mm-thick steel with about 25- μ m-thick zinc coating layer). The filler wire used was AA4043 aluminium series, and the shielding gas used in the coldArc® torch was pure argon. Table 1 summarises the chemical composition of the used materials.

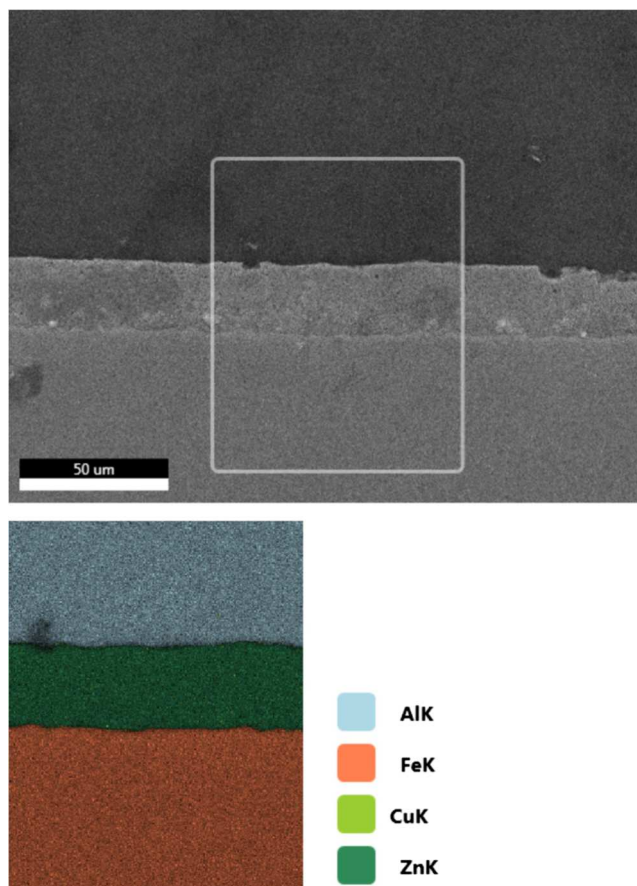
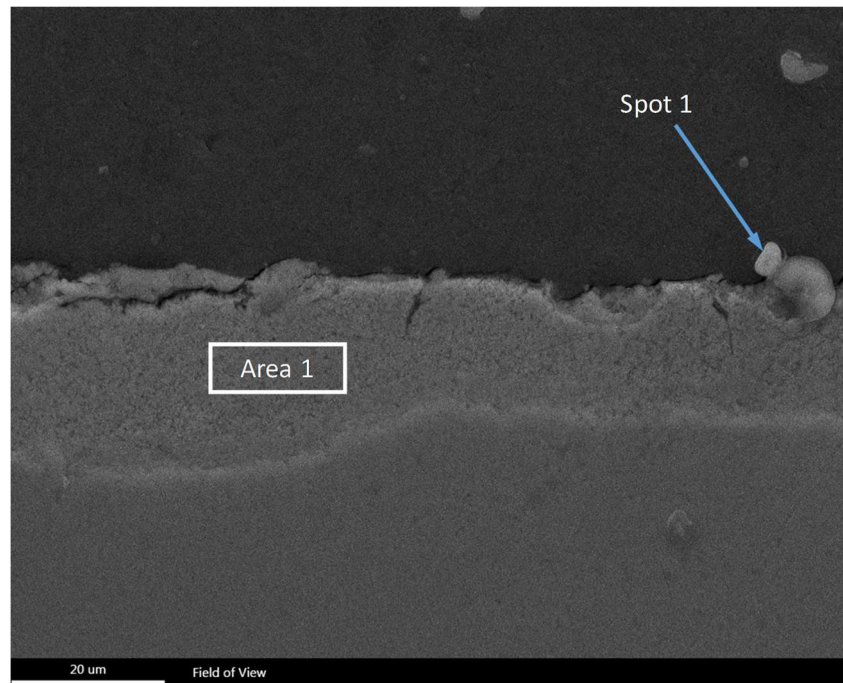


Fig. 5 Map of main metallic elements taken further from melting zone

Fig. 6 Zinc–aluminium interface



As recommended by EWM, for 1 mm thickness, the welding parameters were set as follows: arc voltage 15.3 V, current 54 A and wire feed 5 m/min. All the specimens were manufactured by welding aluminium and steel sheets with a width of 70 mm and then trimmed to 50 mm to remove any unwanted end effect caused by the welding process.

The cruciform welded joints were produced using a welding jig to ensure that the stiffeners are welded as straight as possible and are aligned with the stiffener on the other side. This procedure was essential to reduce the effect of eccentricity. The lap welded joint specimens were produced using a slightly different form than the traditional configuration. The steel sheet was bent at 90°, and the weld took place between the galvanised steel and the aluminium. The reason behind this was that the steel sheets were not galvanised around the edges, and therefore, welding could not be performed directly on the edges themselves.

Table 2 Weight and atomic percentages of elements found in spot 1 and area 1 (Fig. 6)

Element	Weight (%)		Atomic (%)		Error (%)	
	Spot 1	Area 1	Spot 1	Area 1	Spot 1	Area 1
AlK	77.22	2.95	89.05	6.84	6.75	15.38
FeK	1.34	1.07	0.74	1.19	25.98	11.67
CuK	0.14	1.17	0.07	1.15	62.13	18.97
ZnK	21.30	94.82	10.14	90.82	4.96	1.76

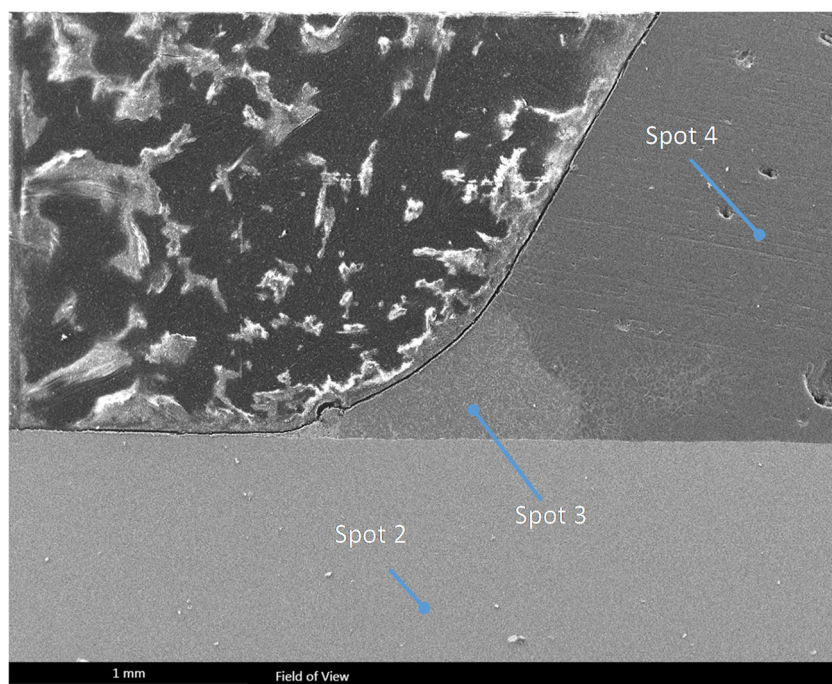
Figure 1a shows the different welded specimens that were tested under tensile static loading to investigate the static strength of aluminium-to-steel welded joints. The tensile tests were run using a 100-kN MAYSE dynamic and static machine. The specimens were prepared as shown in Fig. 1b and tested at room temperature under a nominal displacement rate of 2 mm/min.

4 Metallurgical analysis

A metallurgical investigation of the aluminium-to-steel welded joints was carried out to understand the microstructural behaviour of the joints by performing scanning electron microscopy (SEM) and energy dispersive x-ray (EDX) analyses [20–23]. Figure 4 shows the joint morphology and the position of the investigated sections in the welding zone. The investigated zones were selected to explore different aspects as follows:

- Position a and position b were localised far from the weld zone to analyse the mechanical behaviour and the interaction between the different metallic layers.
- Position c was localised across the joint to analyse the effect of melting at the interface between aluminium, zinc-coated steel and the filler.
- Position d was localised at the interface between the weld and the aluminium sheet.

Fig. 7 Steel–filler interface



The specimens employed for the metallurgical analyses were prepared by using a metallographic cutting machine at room temperature. After that, an ultrasonic device was used to clean the specimens in pure alcoholic solution.

Figure 5 shows what happens during welding at the interface between the aluminium sheet and the galvanised steel sheet (position a, in Fig. 4). Aluminium, steel and zinc layers are presented with a negligible amount of copper found in the zinc layer. By focusing attention on the zinc layer, it is clear that some pores formed within this layer. Looking at Fig. 6, it is apparent that by moving closer to the melting zone (i.e. position b, in Fig. 4), the pores found in the zinc layer have developed into cracks (area 1) and round phases (spot 1) at the interface between the aluminium and the zinc layers. Table 2 presents the chemical compositions of the round particles (spot 1) and around the cracks found in area 1 (Fig. 6). What stands out in this table is the presence of high amounts of zinc (21.3 wt%) in the aluminium alloys, with this implying

the initiation of solid diffusions of the zinc atoms into the aluminium alloy layer. Furthermore, the presence of aluminium particles in the zinc layer (2.95 wt%) suggests that the aluminium atoms have diffused into the zinc layer. The solid diffusion of aluminium and zinc atoms in both layers makes it evident that, although position a and position b are far from the melting zone, there is an improvement of adhesion between the welding sheets.

Fig. 7 explores the interface between the aluminium and the filler. Spot 2 refers to the aluminium sheet, spot 4 refers to the filler and spot 3 is at the interface between the two layers (Table 3). As expected, spots 2 and 4 contain 97.80% of iron and 98.62% of aluminium particles, respectively. However, spot 3 contains 48.41% and 48.59% of aluminium and zinc particles, respectively. This finding

Table 3 Weight percentages of elements found in spots 2, 3 and 4 (Fig. 7)

Element (wt%)	Spot 2	Spot 3	Spot 4
AlK	1.39	48.41	98.62
SiK	0.25	1.54	–
FeK	97.80	1.46	0.47
CuK	0.21	–	0.47
ZnK	0.35	48.59	0.45

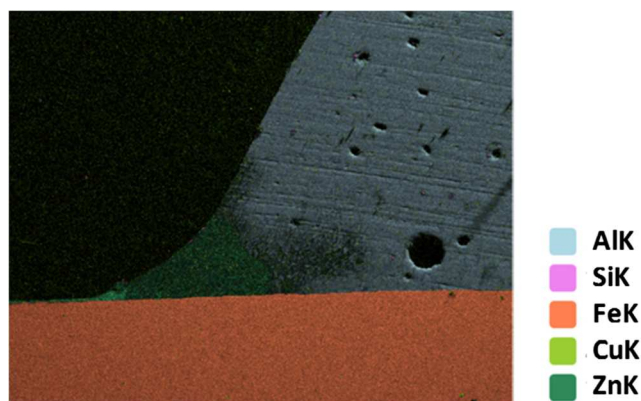


Fig. 8 Distribution of zinc in the filler

Fig. 9 Steel–filler–aluminium interfaces



suggests that during the welding process the zinc particles from the galvanised steel sheet have spread and reacted with the aluminium particles at the interface between the aluminium and filler as seen in Fig. 8.

The area characterised by the presence of all three layers (aluminium, steel and filler) is shown in Fig. 9 and the composition at different places within this area is reported in Table 4. Spot 7 and spot 10 are characterised by the presence of high amounts of aluminium and zinc which determine the start of the joining process between the layers by the metallic inter-diffusion process. Further away from the interface of aluminium and filler layers, the presence of zinc content becomes negligible (spot 6, 8 and 9). By looking at Fig. 10, the presence of zinc in the filler confirms the occurrence of the diffusion mechanism of the zinc particles into the filler.

Table 4 Weight percentages of elements found in spots 5, 6, 7, 8, 9 and 10 (Fig. 9)

Element (wt%)	Spot 5	Spot 6	Spot 7	Spot 8	Spot 9	Spot 10
AlK	0.97	91.56	41.64	98.65	98.62	45.91
SiK	0.19	7.22	6.01	0.56	0.48	2.07
FeK	98.35	0.23	0.43	0.52	0.35	0.24
CuK	0.22	0.26	0.08	0.14	0.28	0.35
ZnK	0.26	0.73	51.84	0.14	0.27	51.43

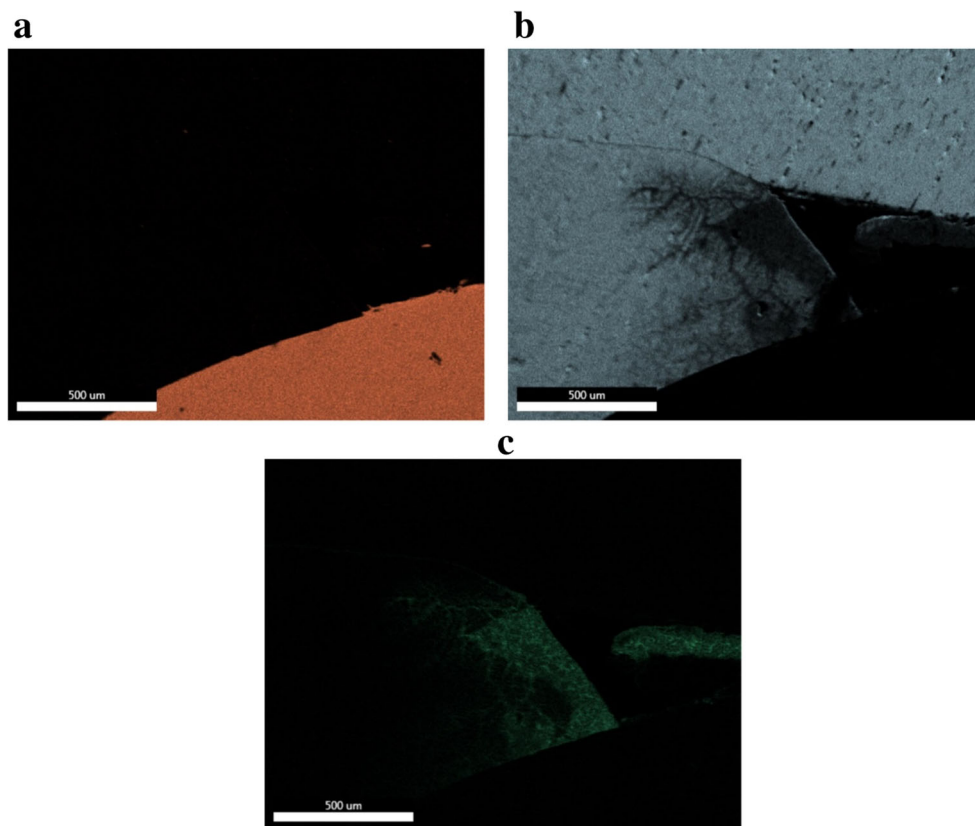
5 Experimental results

The aluminium-to-steel thin welded joints shown in Fig. 1a were tested, in the as-welded condition, under tensile static loading. All the tests were replicated to run two sets of experiments. This exercise was performed to investigate the mechanical performance of the HAZ of the aluminium alloy being tested straightaway after the weld (short-term ageing) and 1 year after welding (long-term ageing).

For each welded configuration being considered, at least nine specimens were tested. Figure 11 shows the measured force (kN) versus extension (mm) data for the different hybrid welded joint geometries. These graphs illustrate how the different types of welded configurations featured a similar behaviour under a tensile static loading. This figure records the maximum forces sustained by the various welded joints. It is noticeable that the force vs. extension response of the hybrid welded joints follows the same force vs. extension behaviour of typical un-welded aluminium alloys. All the samples show a similar behaviour. Tables 5, 6, 7, 8, 9, 10, 11 and 12 summarise the results generated from the tensile experiments for the short-term and long-term specimens. It is clear from the tables that the ultimate tensile strengths show no significant variation and consistent results are achieved by using the EMW coldArc® welding technology.

Figures 12 and 13 present the short-term ageing experimental results obtained from this investigation. These figures summarise the ultimate tensile strength (UTS) for each welded configuration. In particular, Fig. 12 displays

Fig. 10 Map of the main metallic elements in the welding zone: **a** steel, **b** aluminium and **c** zinc



the UTS for butt, lap and cruciform welded joints with \pm two standard deviations from the mean. Figure 13 instead shows the UTS for the single, double and inclined butt welded joints with various inclination angles including 15°, 30°, 45° and 60°. It can be seen from the results in Fig. 13 that, as the weld angle of the hybrid welded joints increased, the static strength increased.

Figure 14a, b displays the fracture surface of the single butt, 15° inclined butt, 30° inclined butt and lap welded joints. For the lap, cruciform, double butt and 45° and 60° inclined butt welded joints, all the samples follow the same fracture behaviour, and the rupture occurs on the aluminium HAZ (Fig. 14a). However, for the single butt, 15° and 30° inclined butt welded joints, there were three different failure modes, including fracture in the aluminium HAZ, fracture through the weld seam and a combination of both failures (Fig. 14b).

Figure 15 compares the results obtained from the short-term and long-term experiments for the single butt, double butt, cruciform and lap welded joints. This figure shows the consistency in strength of the short-term and long-term specimens. Table 13 compares the average UTS for each configuration. There is a small difference between the two sets of experiments, and the effect of long-term ageing can be neglected.

6 Design against static loading

In general, to design any structural component attention must be paid to the weakest part of the structural chain. So, the design resistance of hybrid welded joints should be taken as equal to the design resistance of the weakest part of the connection, in this case, the aluminium part. According to the above experimental findings, Eurocode 9 (EC9) was then used to estimate the static strength of the aluminium-to-steel hybrid welded joint being tested. By using EC9 to design the butt welded and fillet welded joints, the combined stresses and direct stress on the weld throat must be checked and compared with different limiting stresses as shown in Eqs. 1, 2 and 3. Equation 4 is used to design fillet welds.

$$\text{Normal stress : } \sigma_{Ed} \leq \frac{f_w}{\gamma_{Mw}} \quad (1)$$

$$\text{Shear stress : } \tau_{Ed} \leq \frac{1}{\sqrt{3}} \cdot \frac{f_w}{\gamma_{Mw}} \quad (2)$$

$$\text{Normal + Shear stress : } \sigma_{eq} = \sqrt{\sigma_{Ed}^2 + 3\tau_{Ed}^2} \leq \frac{f_w}{\gamma_{Mw}} \quad (3)$$

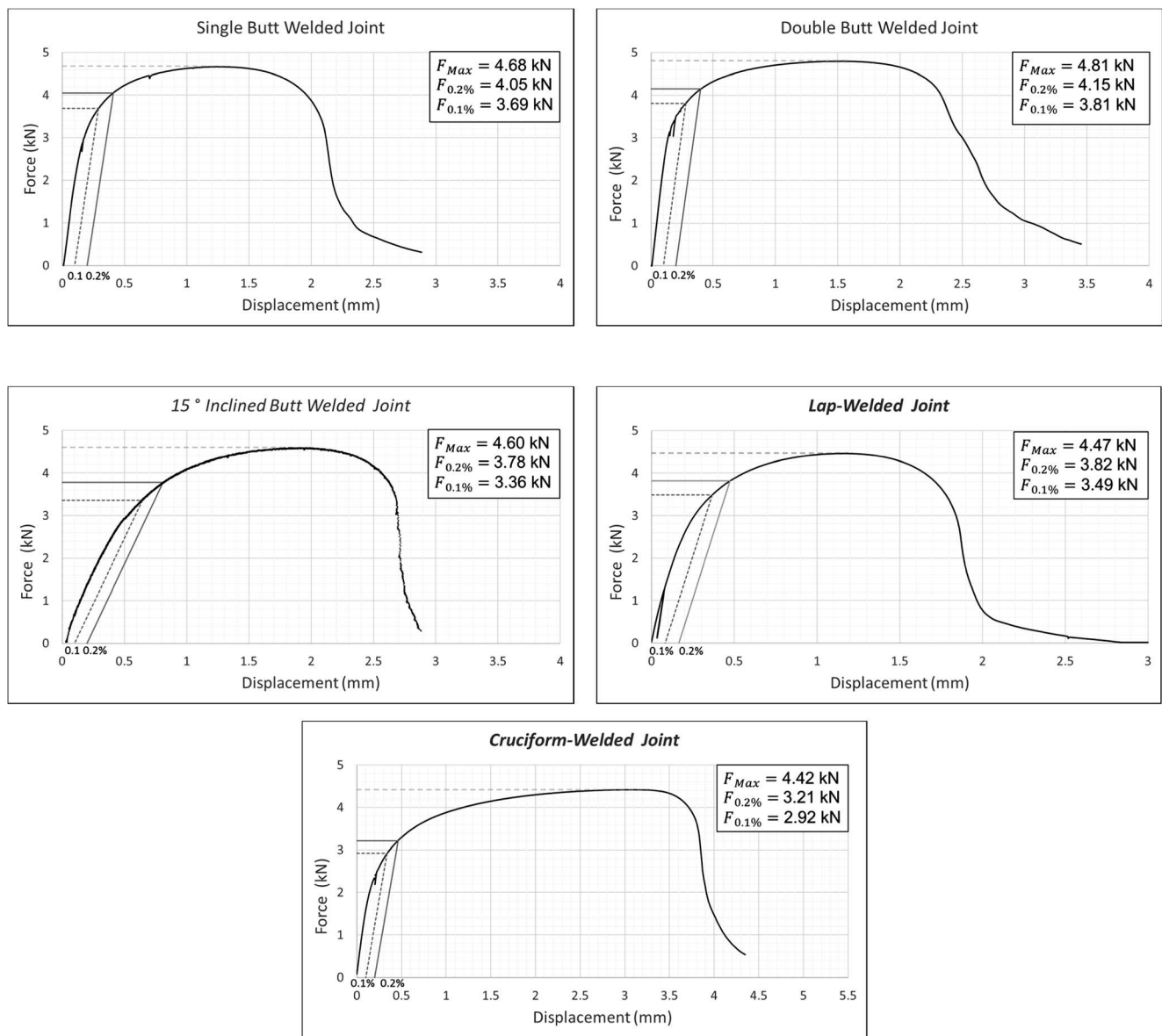


Fig. 11 Force vs. extension for different aluminium-to-steel welded joints

$$\text{Design stress : } \sigma_{eq,fillet} = \sqrt{\sigma_{\perp}^2 + 3(\tau_{\perp}^2 + \tau_{\parallel}^2)} \leq \frac{f_w}{\gamma_{Mw}} \quad (4)$$

According to the British Standard [24], the American Society of Welding [25] and Alves et al. [26], the characteristic strength (f_w) of welded joints made of aluminium alloy AA1050 ranges from 55 to 78 MPa. Figure 16 displays the results obtained by using Eqs. 1, 2, 3 and 4 to design the butt welded specimens (with various weld inclination angles) and the fillet welded joints and compares them with the results from the standard design codes being considered. The results are well above the values suggested by the standard codes, and conservative results are obtained by using EC9 [27]. This fully supports the idea

that aluminium-to-steel welded joints can safely and effectively be designed against static loading by following the assessment procedure recommended by EC9 for aluminium welded joints.

7 Discussion

The results of this study indicate that for the single butt, 15° and 30° inclined butt hybrid joints (reported in Tables 5, 6, 9 and 10), there are three different failure modes: failure occurring in the aluminium HAZ, weld seam fracture and a combination of both failures (see Fig. 14b). There are several explanations for this result. A plausible

Table 5 Ultimate tensile strength of single and double sided butt welded joints (short term)

Code	Angle	Width (mm)	Thickness (mm)	Max tensile load (kN)	UTS (MPa)	Failure mode	
Butt-single-1	0	50.70	1.14	4.68	81	AH	Short-term specimens
Butt-single-2	0	50.64	1.13	4.70	82	AH	
Butt-single-3	0	50.58	1.14	4.57	79	AH	
Butt-single-4	0	50.47	1.14	4.66	81	AH	
Butt-single-5	0	50.34	1.14	3.49	61	WS	
Butt-single-6	0	50.57	1.14	4.73	82	AH	
Butt-single-7	0	50.28	1.14	4.68	82	AH	
Butt-single-8	0	50.35	1.14	4.72	82	AH	
Butt-single-9	0	49.54	1.14	4.67	83	AH	
Butt-single-10	0	50.38	1.13	4.59	81	AH	
Average					79		
Butt-double-1	0	49.24	1.15	4.64	82	AH	
Butt-double-2	0	49.92	1.15	4.67	81	AH	
Butt-double-3	0	50.49	1.14	4.79	83	AH	
Butt-double-4	0	50.55	1.15	4.73	81	AH	
Butt-double-5	0	50.56	1.14	4.39	76	AH	
Butt-double-6	0	50.35	1.14	4.82	84	AH	
Butt-double-7	0	50.68	1.14	4.68	81	AH	
Butt-double-8	0	50.34	1.14	4.39	76	AH	
Butt-double-9	0	50.85	1.14	4.80	83	AH	
Butt-double-10	0	50.31	1.14	4.74	83	AH	
Average					81		

WS weld seam, AH aluminium HAZ

reason for this might be that there is a lack of adhesion between the aluminium and steel as the steel edges are not galvanised. There is already a gap between the two materials, and the weld acts as a bridge between aluminium and steel resulting in the formation of a weak weld. Another explanation for this behaviour is that the weld seam is not thick enough in some specimens resulting in an inadequate weld which can be seen in the second type of failure.

There are, however, other explanation which is that for some specimens the quality of the weld is inadequate. This can be seen clearly in the third failure mode where the crack initiates and start propagating from the weld seams until it hits a strong weld then it diverges its path and starts propagating on the aluminium HAZ. There are ways to solve this problem, either by galvanising the edges of the steel sheet or by using different geometries where the edges of the steel are galvanised. Another solution is to use automated welding machine to obtain a consistent weld thickness along the weld path.

The results reported in Tables 5 and 9 for the double butt joints indicate that the fracture of the joints always took place in the aluminium HAZ. These results confirm the association between the thickness of the weld seams

and the strength of the weld. Although there is still a gap between the two materials, having welded on both sides increased the strength of the welds themselves. This overcomes the problem of having a fracture on the weld seam.

For double butt, 45°, 60° inclined butt, cruciform and lap welded joints, the fracture always took place in the aluminium HAZ away from the weld seam (see Fig. 14a). These findings demonstrate that the use of the EWM coldArc® technology improved the strength of the aluminium-to-steel hybrid welded joints significantly and successfully dealt with the problem of having a brittle phase in the welding zone. The use of low heat input reduced the size of the intermetallic phase at the weld interface which resulted in a stronger weld.

From Fig. 12, it is worth mentioning that the same static strength is achieved both for single butt and double butt welded joints. This finding further confirms that, for the combination of materials being investigated, the welded joints manufactured via the EWM coldArc® welding technology were stronger than the heat-affected zone in the aluminium alloys. In particular, the UTS of the aluminium HAZ of the butt, lap and cruciform welded joints was seen to be larger than 70% of the parent

Table 6 Ultimate tensile strength of single-sided butt welded joints with various inclination angles (short term)

Code	Angle	Width (mm)	Thickness (mm)	Max tensile load (kN)	UTS (MPa)	Failure mode	
Butt-single-1	15	50.07	1.14	4.82	84	AH	Short-term specimens
Butt-single-2	15	50.27	1.15	4.77	83	AH	
Butt-single-3	15	50.28	1.14	4.88	85	AH	
Butt-single-4	15	50.11	1.15	3.83	66	WS	
Butt-single-5	15	50.06	1.14	4.43	78	AH/WS	
Butt-single-6	15	50.48	1.14	4.07	71	WS	
Butt-single-7	15	50.47	1.14	4.82	84	AH	
Butt-single-8	15	50.14	1.14	2.81	49	WS	
Butt-single-9	15	50.22	1.13	3.28	58	WS	
Butt-single-10	15	50.21	1.14	4.47	78	AH/WS	
Average					74		
Butt-single-1	30	50.35	1.15	3.88	67	AH/WS	
Butt-single-2	30	50.13	1.14	5.04	88	AH	
Butt-single-3	30	50.32	1.14	5.08	89	AH	
Butt-single-4	30	50.15	1.14	5.10	89	AH	
Butt-single-5	30	50.47	1.14	5.02	87	AH	
Butt-single-6	30	50.34	1.14	5.00	87	AH	
Butt-single-7	30	49.89	1.14	4.67	82	AH	
Butt-single-8	30	50.27	1.15	4.86	84	AH	
butt-single-9	30	50.17	1.14	5.06	88	AH	
Average					85		
Butt-single-1	45	50.55	0.98	5.15	104	AH	
Butt-single-2	45	49.83	0.99	4.95	100	AH	
Butt-single-3	45	50.66	0.99	4.66	93	AH	
Butt-single-4	45	50.76	1.00	5.43	107	AH	
Butt-single-5	45	50.63	1.00	5.58	110	AH	
Butt-single-6	45	50.32	0.99	4.92	99	AH	
Butt-single-7	45	50.81	0.98	4.92	99	AH	
Butt-single-8	45	50.62	0.99	5.03	100	AH	
Butt-single-9	45	50.15	0.99	4.94	99	AH	
Average					101		
Butt-single-1	60	50.46	0.99	5.24	105	AH	
Butt-single-2	60	49.76	0.99	5.64	114	AH	
Butt-single-3	60	50.59	1.00	5.56	110	AH	
Butt-single-4	60	50.64	0.99	5.82	116	AH	
Butt-single-5	60	50.68	0.99	5.32	106	AH	
Butt-single-6	60	50.37	0.99	5.53	111	AH	
Butt-single-7	60	50.53	0.99	5.22	104	AH	
Butt-single-8	60	50.55	0.99	5.46	109	AH	
Butt-single-9	60	50.28	0.99	5.10	102	AH	
Butt-single-10	60	50.48	0.98	5.35	108	AH	
Average					109		

WS weld seam, AH aluminium HAZ

aluminium UTS. These findings fully confirm that aluminium-to-steel hybrid welded joints with excellent mechanical performance can be manufactured using the EWM coldArc® welding technology.

The results in Fig. 16 confirm that EC9 recommendations along with a characteristic strength value for the welded aluminium alloys provide a suitable design

Table 7 Ultimate tensile strength of lap welded joints (short term)

Code	Angle	Width (mm)	Thickness (mm)	Max tensile load (kN)	UTS (MPa)	Failure mode	
Lap-1	0	48.72	1.00	4.48	92	AH	Short-term specimens
Lap-2	0	49.35	0.99	4.45	91	AH	
Lap-3	0	49.27	1.01	4.45	89	AH	
Lap-4	0	49.49	1.01	4.48	90	AH	
Lap-5	0	49.37	1.01	4.41	88	AH	
Lap-6	0	49.49	1.02	4.50	89	AH	
Lap-7	0	49.75	1.00	4.46	90	AH	
Lap-8	0	49.26	1.00	4.47	91	AH	
Lap-9	0	49.55	0.99	4.38	89	AH	
Lap-10	0	49.43	1.01	4.47	90	AH	
Lap-11	0	49.45	1.00	4.51	91	AH	
Lap-12	0	49.68	1.00	4.56	92	AH	
Lap-13	0	49.59	1.01	4.48	89	AH	
Average					90		

WS weld seam, AH aluminium HAZ

approach for aluminium-to-steel hybrid welded joints against static loading.

Finally, by performing short-term and long-term ageing experiments, it is evidently clear from the findings that ageing has little or no effect on the tensile strength of the welded joints. These results suggest that the strength of the heat-affected zone of the aluminium alloys has already recovered from the welding process and therefore leaving the specimens for a longer period would lead to similar results.

8 Conclusion

This study provides the first comprehensive assessment of the static strength of aluminium-to-steel thin welded joints using the EWM coldArc® welding technology. The key findings of this research project have been the following:

- The use of the EWM coldArc® welding technology results in efficient and robust aluminium-to-steel

Table 8 Ultimate tensile strength of cruciform welded joints (short term)

Code	Angle	Width (mm)	Thickness (mm)	Max tensile load (kN)	UTS (MPa)	Failure mode	
Cr-1	0	50.28	1.03	4.46	86	AH	Short-term specimens
Cr-2	0	48.99	1.02	4.35	87	AH	
Cr-3	0	49.80	1.03	4.44	87	AH	
Cr-4	0	50.11	1.02	4.18	82	AH	
Cr-5	0	49.28	1.00	4.40	89	AH	
Cr-6	0	49.63	1.01	4.37	87	AH	
Cr-7	0	49.42	1.00	4.41	89	AH	
Cr-8	0	49.37	1.01	4.42	89	AH	
Cr-9	0	49.30	1.01	4.38	88	AH	
Cr-10	0	49.89	1.01	4.59	91	AH	
Cr-11	0	51.14	1.02	4.52	87	AH	
Average					87		

WS weld seam, AH aluminium HAZ

Table 9 Ultimate tensile strength of single and double sided butt welded joints (long term)

Code	Angle	Width (mm)	Thickness (mm)	Max tensile load (kN)	UTS (MPa)	Failure mode	
Butt-single-1	0	50.76	1.14	3.99	69	WS	Long-term specimens
Butt-single-2	0	60.00	1.13	4.44	65	WS	
Butt-single-3	0	50.60	1.14	4.87	84	AH	
Butt-single-4	0	50.65	0.98	4.37	88	WS	
Butt-single-5	0	51.11	1.14	4.95	85	AH	
Butt-single-6	0	50.71	1.14	4.95	86	WS	
Butt-single-7	0	50.96	1.14	3.44	59	WS	
Butt-single-8	0	50.25	1.14	4.73	83	AH/WS	
Butt-single-9	0	50.45	1.14	4.90	85	AH	
Butt-single-10	0	50.49	1.13	3.99	70	WS	
Average					77		
Butt-double-1	0	53.15	1.15	5.23	86	AH	
Butt-double-2	0	50.34	1.15	4.77	82	AH	
Butt-double-3	0	50.68	1.13	4.84	85	AH	
Butt-double-4	0	50.47	1.14	4.95	86	AH	
Butt-double-5	0	49.98	1.15	4.81	84	AH	
Butt-double-6	0	49.12	1.15	4.76	84	AH	
Butt-double-7	0	49.10	1.14	4.80	86	AH	
Butt-double-8	0	50.63	1.15	4.84	83	AH	
Butt-double-9	0	53.15	1.15	4.90	80	AH	
Average					84		

WS weld seam, AH aluminium HAZ

Table 10 Ultimate tensile strength of single-sided butt welded joints with various inclination angles (long term)

Code	Angle	Width (mm)	Thickness (mm)	Max tensile load (kN)	UTS (MPa)	Failure mode	
Butt-single-1	15	50.33	1.14	5.05	88	AH	Long-term specimens
Butt-single-2	15	50.31	1.15	3.58	62	WS	
Butt-single-3	15	50.49	1.15	3.77	65	WS	
Butt-single-4	15	48.15	1.15	4.76	86	AH	
Butt-single-5	15	50.21	1.15	3.71	64	WS	
Butt-single-6	15	50.26	1.15	4.70	81	AH/WS	
Butt-single-7	15	50.38	1.15	4.54	78	WS	
Butt-single-8	15	50.04	1.14	4.94	87	AH	
Butt-single-9	15	50.57	1.14	4.16	72	AH/WS	
Butt-single-10	15	50.12	1.15	4.99	87	AH	
Butt-single-11	15	50.26	1.14	5.00	87	AH	
Average					78		
Butt-single-1	30	50.65	1.12	5.33	94	AH	
Butt-single-2	30	50.29	1.14	5.23	91	AH	
Butt-single-3	30	50.26	1.14	5.25	92	AH	
Butt-single-4	30	50.09	1.15	5.17	90	AH	
Butt-single-5	30	50.33	1.14	5.11	89	AH/WS	
Butt-single-6	30	50.76	1.15	4.88	84	AH/WS	
Butt-single-7	30	50.65	1.15	4.99	86	AH/WS	
Butt-single-8	30	50.13	1.15	4.85	84	AH	

Table 10 (continued)

Code	Angle	Width (mm)	Thickness (mm)	Max tensile load (kN)	UTS (MPa)	Failure mode
Butt-single-9	30	50.47	1.15	5.24	90	AH/WS
Butt-single-10	30	49.44	1.15	5.33	94	WS
Butt-single-11	30	50.41	1.15	5.26	91	AH
Average					89	
Butt-single-1	45	50.66	0.98	4.97	100	AH
Butt-single-2	45	50.76	0.99	5.27	105	AH
Butt-single-3	45	50.93	0.99	5.37	107	AH
Butt-single-4	45	50.92	0.99	5.25	104	AH
Butt-single-5	45	50.25	0.99	5.16	104	AH
Butt-single-6	45	50.83	0.99	5.14	102	AH
Butt-single-7	45	50.89	1.00	4.95	97	AH
Butt-single-8	45	50.10	1.00	5.52	110	AH
Butt-single-9	45	50.59	0.99	5.11	102	AH
Butt-single-10	45	50.69	0.98	5.08	102	AH
Average					103	
Butt-single-1	60	50.65	1.00	5.59	110	AH
Butt-single-2	60	50.26	1.00	5.81	116	AH
Butt-single-3	60	50.59	1.00	5.35	106	AH
Butt-single-4	60	50.59	1.00	5.59	110	AH
Butt-single-5	60	50.53	1.00	4.97	98	AH
Butt-single-6	60	50.08	1.00	5.23	104	AH
Butt-single-7	60	50.57	1.00	5.51	109	AH
Butt-single-8	60	50.24	1.00	5.69	113	AH
Butt-single-9	60	50.77	0.99	5.69	113	AH
Average					109	

WS weld seam, AH aluminium HAZ

Table 11 Ultimate tensile strength of lap welded joints (long term)

Code	Angle	Width (mm)	Thickness (mm)	Max tensile load (kN)	UTS (MPa)	Failure mode
Lap-1	0	49.83	1.00	4.48	90	AH
Lap-2	0	49.24	1.01	4.45	89	AH
Lap-3	0	49.20	1.00	4.45	90	AH
Lap-4	0	49.38	0.99	4.49	92	AH
Lap-5	0	49.42	1.00	4.42	89	AH
Lap-6	0	49.46	1.00	4.51	91	AH
Lap-7	0	49.24	1.00	4.48	91	AH
Lap-8	0	49.42	1.00	4.48	91	AH
Lap-9	0	49.37	1.00	4.39	89	AH
Lap-10	0	49.98	1.00	4.48	90	AH
Lap-11	0	50.17	0.99	4.51	91	AH
Average					90	

WS weld seam, AH aluminium HAZ

Table 12 Ultimate tensile strength of cruciform welded joints (long term)

Code	Angle	Width (mm)	Thickness (mm)	Max tensile load (kN)	UTS (MPa)	Failure mode
Cr-1	0	50.06	1.00	4.80	96	AH
Cr-2	0	50.55	1.00	4.62	91	
Cr-3	0	50.11	1.00	4.60	92	
Cr-4	0	50.31	1.00	4.67	93	
Cr-5	0	50.75	0.99	4.66	93	
Cr-6	0	49.91	1.01	4.65	92	
Cr-7	0	50.90	1.00	4.57	90	
Cr-8	0	50.00	1.00	4.56	91	
Cr-9	0	49.96	1.00	4.66	93	
Cr-10	0	50.60	1.00	4.64	92	
Average					92	

WS weld seam, AH aluminium HAZ

Fig. 12 The average tensile strength results of Al-St butt, lap and cruciform welded joints (short-term ageing)

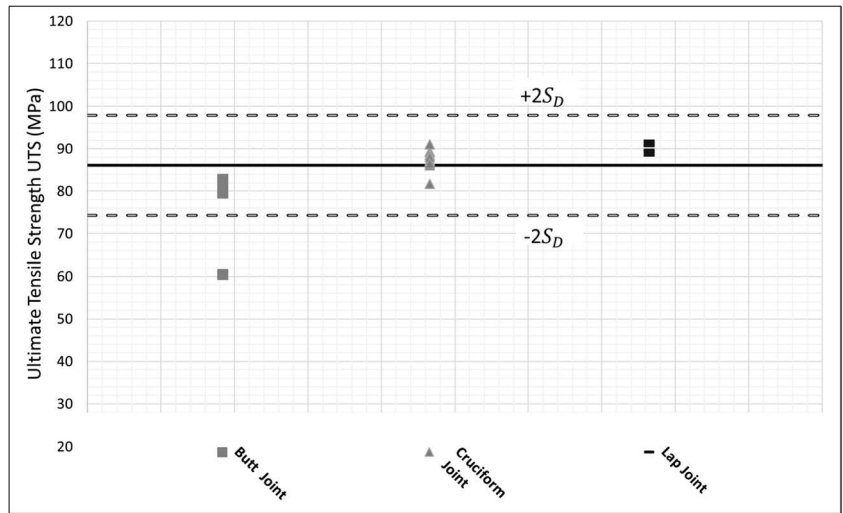
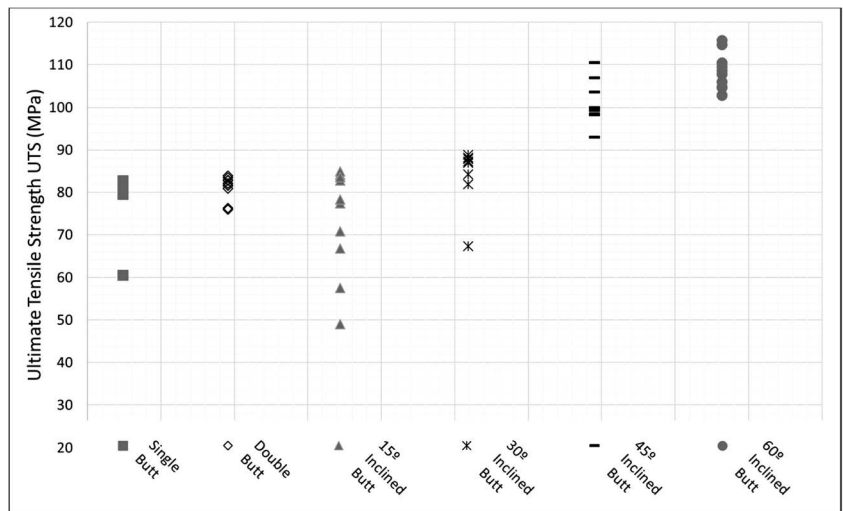


Fig. 13 The average tensile strength results of Al-St butt welded joints with various inclination angles (short-term ageing)



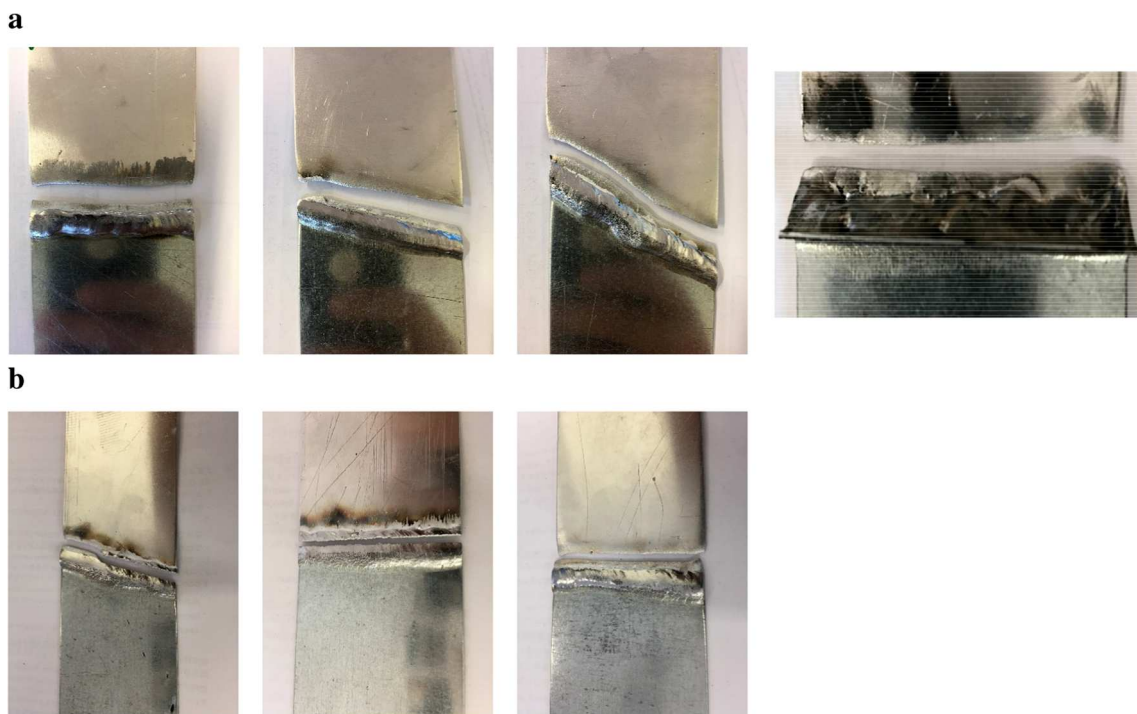


Fig. 14 Tensile static failure of double butt, 45° and 60° inclined butt, cruciform and lap hybrid welded joints (a). Tensile static failure modes of single butt, 15° and 30° inclined butt hybrid welded joints (b)

- welded joints, with the manufacturing requiring minimum effort.
- Irrespective of the configuration or inclination angle of the hybrid welded joints, the fracture failure will always occur on the aluminium side.
- The results generated by testing our specimens confirm that aluminium-to-steel welded joints can be designed against static loading by focussing attention solely on the aluminium part, i.e. on the weakest link in the structural chain of the joint.

Fig. 15 Comparison between the short-term and long-term tensile static strength of butt welded, cruciform welded and lap welded aluminium-to-steel hybrid joints

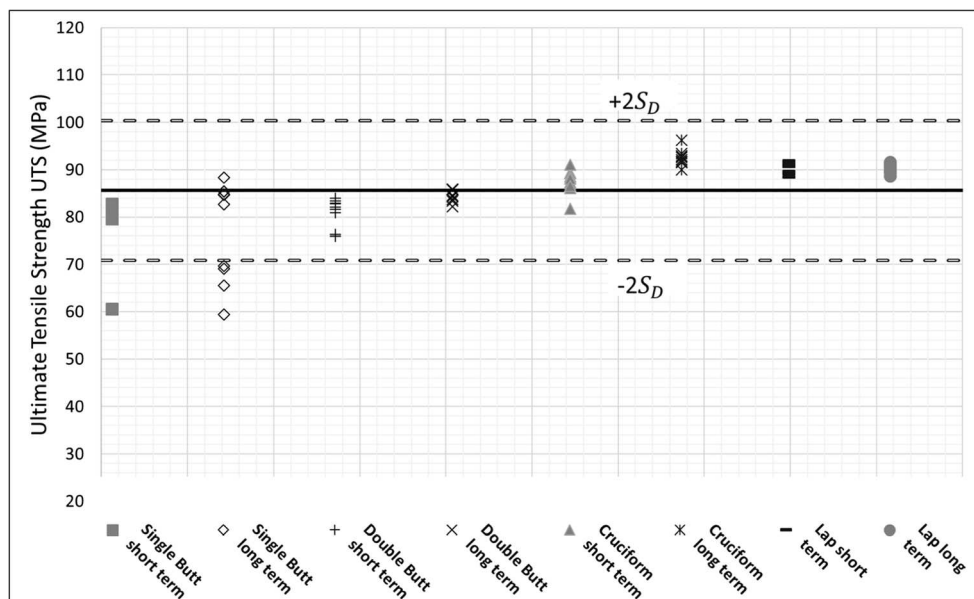
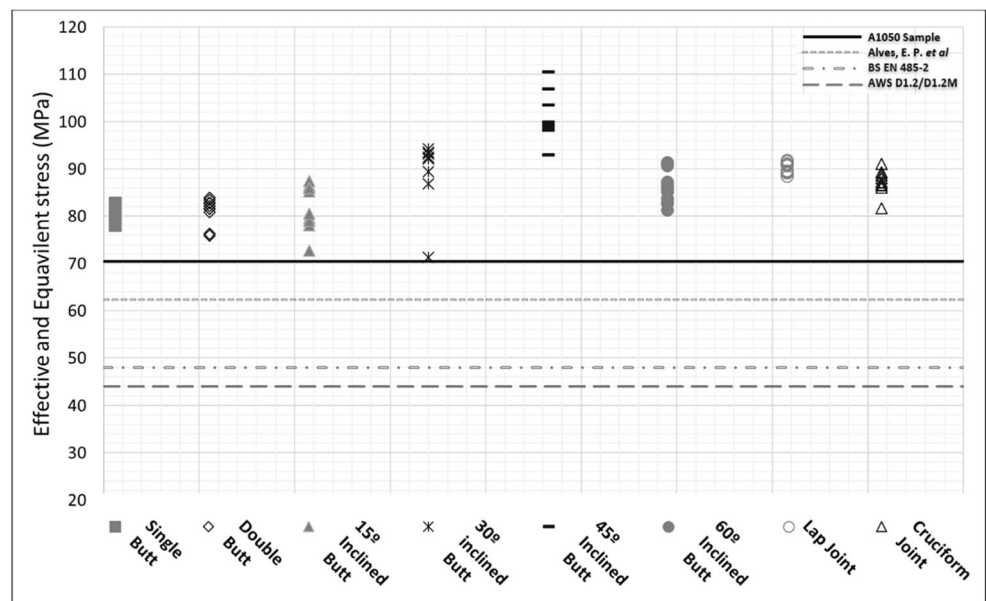


Table 13 Ultimate tensile strength comparison of the short-term and long-term experiments

Configuration type	Angle	Average UTS (MPa)	
		Short term	Long term
Butt-single	0	79	77
Butt-double	0	81	84
Butt-single	15	74	78
Butt-single	30	85	89
Butt-single	45	101	103
Butt-single	60	109	109
Lap	0	90	90
Cruciform	0	87	92

Fig. 16 Effective and equivalent design stresses of aluminium-to-steel welded joints compared with standard design codes

Acknowledgements EWM® (www.ewm-group.com) is acknowledged for supporting the present research investigation.

Open Access This article is distributed under the terms of the Creative Commons Attribution 4.0 International License (<http://creativecommons.org/licenses/by/4.0/>), which permits unrestricted use, distribution, and reproduction in any medium, provided you give appropriate credit to the original author(s) and the source, provide a link to the Creative Commons license, and indicate if changes were made.

References

- Kimapong K, Watanabe T (2005) Lap joint of A5083 aluminium alloy and SS400 steel by friction welding. *Mater Trans* 46(4):835–841
- Meco S, Pardal G, Ganguly S, Williams S, McPherson N (2015) Application of laser in seam welding of dissimilar steel to aluminium joints for thick structural components. *Opt Laser Eng* 67:22–30
- QIN G, SU Y, WANG S (2004) Microstructures and properties of welded joint of aluminium alloy to galvanized steel by Nd: YAG laser + MIG arc hybrid brazing-fusion welding. *Trans Nonferrous Metals Soc China* 24:989–995
- Chao R, Yang J, Lay S (1997) Interfacial toughness for the ship-board aluminium/steel structural transition joint. *Mar Struct* 10: 353–362
- McKenney C, Banker J (1971) Explosion-bonded metals for marine structural applications. *Mar Technol* 5(7):285–292
- Okamura H, Aota K (2004) Joining of dissimilar materials with friction stir welding. *Weld Int* 18(11):852–860
- Katayama S (2004) Laser welding of aluminium alloys and dissimilar metals. *Weld Int* 18(8):618–625
- Kato K, Tokisue H (2004) Dissimilar friction welding of aluminium alloys to other materials. *Weld Int* 18(11):861–867

9. Lu Z, Huang P, Gao W, Li Y, Zhang H, Yin S (2009) ARC welding method for bonding steel with aluminium. *Front Mech Eng China* 4(2):134–143
10. Fukumoto S, Tsubakino H, Okita K, Aritoshi M, Tomita T (1999) Friction welding process of 5052 aluminium alloy to 304 stainless steel. *Mater Sci Technol* 15(9):1080–1086
11. Elrefaey A, Gouda M, Takahashi M, Ikeuchi K (2005) Characterization of aluminium/steel lap joint by friction stir welding. *J Mater Eng Perform* 14(1):12–17
12. Liu H, Maeda M, Fujii H, Nogi K (2003) Tensile properties and fracture locations of friction-stir welded joints of 1050-H24 aluminium alloy. *J Mater Sci Lett* 22:41–43
13. Leitao C, Arruti E, Aldanondo E, Rodrigues D (2016) Aluminium-steel lap joining by multipass friction stir welding. *Mater Des* 106:153–160
14. Wang P, Chen X, Pan Q, Madigan B, Long J (2016) Laser welding dissimilar materials of aluminum to steel: an overview. *Int J Adv Manuf Technol* 87:3081–3090
15. Gao M, Chen C, Mei S, Wang L, Zeng X (2014) Parameter optimization and mechanism of laser-arc hybrid welding of dissimilar Al alloy and stainless steel. *Int J Adv Manuf Technol* 74:199–208
16. Era T, Isw A, Uezono T, Ueyama T, Hitata Y (2013) Controlled bridge transfer (CBT) gas metal arc process for steel sheets joining. *Weld Int* 27(4):268–273
17. Cao R, Sun JH, Chen JH, Wang P (2014) Cold metal transfer joining aluminum alloys-to-galvanized mild steel. *J Manuf Sci Eng* 136:051015-1–051015-10
18. Goecke SF (2005) Low energy arc joining process for materials sensitive to heat. EWM, Mündersbach. <https://www.industrialsolutions-llc.com/resources/downloads/ewm-coldarcbrochure-detailed.pdf>. Accessed 8 Aug 2018
19. Kah P, Suoranta R, Martikainen J (2013) Advanced gas metal arc welding processes. *Int J Adv Manuf Technol* 67:655–674
20. Goldstein J, Newbury DE, Joy DC, Lyman CE, Echlin P, Lifshin E, Sawyer L, Michael JR (2003) *Scanning electron microscopy and X-ray microanalysis*, 3rd edn. Springer, New York
21. Scott VD, Love G (1994) *Quantitative electron probe microanalysis*, 2nd edn. Ellis Horwood, Chichester
22. Reed SJB (1993) *Electron microprobe analysis*, 2nd edn. Cambridge University Press, Cambridge
23. Agarwal BK (1991) *X-ray spectroscopy*, 2nd edn. Springer-Verlag, Berlin
24. BS EN 485-2:2016 (2016) Aluminium and aluminium alloys—sheet, strip and plate—part 2: mechanical properties. European Committee for Standardization, British Standards Institution, London
25. AWS D1.2/D1.2M:2014 (2014) *Structural welding code—aluminium*. American Welding Society, USA
26. Alves EP, Neto FP, An CY (2010) Welding of AA1050 aluminum with AISI 304 stainless steel by rotary friction welding process. *J Aerosp Technol Manag* 2(3):301–306
27. Eurocode 9 (1998) *Design of aluminium structures—part 1-1: general structural rules*, prENV